Evidence for a Direct Manganese−Oxygen Ligand in Water Binding to the S_2 State of the Photosynthetic Water Oxidation Complex†

M. C. W. Evans,*,‡ J. H. A. Nugent,‡ R. J. Ball,‡ I. Muhiuddin,‡ and R. J. Pace§

Department of Biology, University College London, Gower Street, London WC1E 6BT, U.K., and Department of Chemistry, Faculty of Science, Australian National University, Canberra, ACT 0200, Australia

Received August 20, 2003; Revised Manuscript Received December 3, 2003

ABSTRACT: The interaction of water with the water oxidizing Mn complex of photosystem II has been investigated using electron spin−echo envelope modulation spectroscopy in the presence of $H_2{}^{17}O$. The spectra show interaction of the ^{17}O with the preparation in the S_2 state induced by 200 K illumination. The modulation is observed only in the center of the multiline spectrum. The inferred hyperfine coupling terms are compatible with water (not hydroxyl) oxygen bound to a particular quasi-axial Mn^{III} center in a coupled Mn cluster.

The oxidation of water in photosynthesis is catalyzed by a membrane-bound reaction center complex, photosystem II. Water oxidation depends on a complex Mn center that functions as an oxidant accumulator and is thought to provide the catalytic site for water oxidation (for reviews see ref *1*). Classical experiments (*2*, *3*) show that the evolution of oxygen following single turnover flash illumination of photosystem II occurs on the third flash and, subsequently, on every fourth flash. This process is formalized in the S state hypothesis. This requires an oxidant accumulation complex that has five formal redox states, S_0-S_4. The dark stable resting state is S_1. Each turnover of the reaction center advances the oxidation state of the complex from S_0 to S_4; the oxidation of water and release of oxygen then occurs rapidly in the dark, returning the complex to S_0.

Mn is an essential component of the water oxidation complex. It is well established that in eukaryotic photosystem II the Mn complex contains μ-oxo-bridged pairs and that pairs in two different orientations to the membrane plane can be characterized by EXAFS[1] (*1*, *4*, *5*). Both X-ray and EPR spectroscopy can detect changes in the oxidation state of the Mn complex, clearly indicating that the complex is the oxidant accumulator for water oxidation. The S_0 (*6*−*8*) and S_2 (*9*) states have complex multiline EPR spectra detectable in standard perpendicular mode EPR. The S_1 and S_3 states are normally considered to be EPR silent but have been shown to have integer spin signals detectable in parallel mode EPR (*10*, *11*).

The mechanism of water oxidation is still unknown. Although many models have been suggested, the site of water binding and oxidation has not been unequivocally identified. Identification of the Mn complex as the oxidant accumulator has provided support for the proposal that it is also the catalytic site. However, it has proved difficult to obtain strong evidence for water binding to the Mn.

The work of Wydrzynski and co-workers (*12*, *13*) indicates that water is bound to the water oxidation complex in S_1 but remains exchangeable until S_3. They detect two rates of exchange indicating two sites of water binding, one significantly stronger than the other. Characterization of EPR signals for the S_0 and S_2 states offers the possibility of identifying interaction of substrates with the Mn complex detecting the interaction of magnetic nuclei with the electron spin giving rise to the multiline signal using either ^2H- or ^{17}O-labeled water. Two attempts to detect binding using CW EPR have been reported. Andreasson (*14*) identified small changes in the multiline signal using $H_2{}^{17}O$. Nugent (*15*) also reported small changes in ^2H_2O, but the latter may be reinterpreted as reflecting the overall exchange of deuterons into the proteins of the complex. The pulsed EPR ESEEM technique offers a much more specific way to detect interaction of ^{17}O or ^2H with the Mn complex, either through direct ligand formation or interaction with nuclei in the close environment of the center. We reported the use of ESEEM spectroscopy to investigate interactions in the S_1 and S_2 states with ^2H_2O and $H_2{}^{17}O$ (*16*). In those experiments we were unable to detect any specific or strong interaction that could be assigned to water interaction with the Mn complex. However, subsequently we (*17*) and Britt and co-workers (*18*) showed that interaction of small alcohols, particularly methanol binding, with the S_2 state could be detected. We found that this interaction was only seen in freshly prepared S_2 samples. The modulated signals decayed over a relatively short time during storage at liquid nitrogen temperatures, although a large part of the multiline signal was stable. Further work then showed that very strong modulation by deuterium in ^2H_2O associated with the metastable S_2 multiline

† This work was supported in part by grants from the U.K. Biotechnology and Biological Sciences Research Council. R.J.P. acknowledges support from the Australian Research Council.

* Corresponding author. Phone: +44-207-679-7312. Fax: +44-207-679-7098. E-mail: mcw.evans@ucl.ac.uk.

‡ University College London.

§ Australian National University.

[1] Abbreviations: EPR, electron paramagnetic resonance; ESE, electron spin−echo; ESEEM, electron spin−echo envelope modulation; CW, continuous wave; EPR, electron paramagnetic resonance; EXAFS, X-ray absorption fine structure; XANES, X-ray absorption near-edge spectra; FT, Fourier transform; Q_A, the first quinone electron acceptor in the photosystem II reaction center.

10.1021/bi035489y CCC: $27.50
Published on Web 01/08/2004

signal could be detected (*19*, *20*). This indicated close approach of water to the Mn complex in the S_1 state, as the S_2 state was generated by 200 K illumination of samples frozen in S_1, conditions where water movement is restricted. The ^2H modulation was shown to be associated with a narrow form of the multiline signal. The existence of two forms of the multiline signal had previously been identified in several laboratories (*21*, *22*), while the existence of two environments for Mn atoms and different effects of S state oxidation in each environment had been shown by X-ray spectroscopy (*4*, *5*).

The experiments with ^2H_2O, while showing very strong modulation, do not provide conclusive evidence for the binding of water to the Mn, but they do show the presence of readily exchangeable protons in the immediate vicinity of the Mn. We have now repeated the experiments using ^{17}O-labeled water to determine if the direct binding of water to the Mn complex can be demonstrated.

MATERIALS AND METHODS

Sample Preparation. PSII membranes were prepared from 10 to 14 day old pea seedlings using Triton X-100, using the modifications of Ford and Evans (*23*). Reagents used were all of analytical grade. Chlorophyll concentration was measured by the method of Porra (*24*). Control rates of oxygen evolution for PSII membranes were 500−1100 μmol of O_2 (mg of Chl)$^{-1}$ h^{-1} using ferricyanide and dimethylbenzoquinone as electron acceptors and were measured in an oxygen electrode at 298 K. The membranes were stored at 77 K in 20 mM 2-(*N*-morpholino)ethanesulfonic acid, 15 mM NaCl, 5 mM $MgCl_2$, and 0.4 M sucrose, pH 6.3 (buffer A). Before preparation of EPR samples, the PSII membranes were (except where stated) washed in buffer A containing 2 mM ethylenediaminetetraacetic acid to remove adventitiously bound Mn^{2+}, followed by centrifugation and resuspension in buffer A. Preparations were transferred into $H_2{}^{17}O$ by centrifuging the preparation from the $H_2{}^{16}O$ medium and resuspending into $H_2{}^{17}O$ 35−40% enriched with ^{17}O. In an attempt to increase the final enrichment one preparation was resuspended in buffer A made by adding 50 times concentrated buffer A to the $H_2{}^{17}O$, centrifuging the sample, and resuspending again into buffer A. The spectra shown were obtained with this preparation. Overall, five different preparations were used with two or three matching samples from each preparation. No obvious differences were observed in the spectra from different preparations.

For EPR, 0.3−0.4 mL samples (approximately 6−10 mg of chlorophyll/mL; 25−40 μM photosystem II) were placed in calibrated ~3 mm quartz EPR tubes. Matching sets of samples in $H_2{}^{16}O$ and $H_2{}^{17}O$ in calibrated EPR tubes were made for each experiment, using the same preparation and chlorophyll concentration. They were given a brief (30 s) illumination at 277 K to turn over the photosystem II reaction center and restore the $Y_D^{\bullet}$ lost on storage. Further procedures were carried out in the dark or under a dim green light. Samples were prepared as in ref *16* except that 1 mM phenyl-*p*-benzoquinone replaced dimethylbenzoquinone.

Samples were dark adapted for 3.5−4 h at 273 K and then treated as described in the text and figure legends. This produced samples initially in the S_1 Q_A state, as indicated by the absence of the S_2 EPR markers, the multiline signal, or the $g = 4.1$ signal, and $Q_A^{\bullet-}$. Absence of photosystem I was confirmed by the lack of signals from oxidized P700 or reduced iron−sulfur centers A or B following illumination at <30 K.

EPR. Samples were examined by CW EPR at cryogenic temperatures using a JEOL RE1X spectrometer fitted with an Oxford Instruments cryostat to confirm the formation of the multiline signal. Samples were illuminated at 200 K using a 1000 W light source, protecting the sample from heating where necessary by a 5 cm water filter. Samples were maintained at 200 K during illumination in an ethanol/dry ice bath in an unsilvered clear glass dewar. The temperature of the bath was measured by thermometer. Samples were annealed by thawing in the dark at 275 K for 30 s, mixing, and then refreezing to 77 K (taking 60−75 s total time) (*25*).

ESEEM spectra were recorded on a Bruker ESP380E X-band pulsed spectrometer equipped with a Bruker 1052 DLQ-H8907 variable Q dielectric resonator and an Oxford Instruments CF395 cryostat. ESEEM spectra were recorded as in Turconi et al. (*15*). A three-pulse $p-\tau-p-T-p-$echo phase-cycled sequence generated a stimulated ESEEM spectrum where τ is set and T is varied. All ESEEM spectra were recorded with a cavity Q of about 100 resulting in a minimum cavity dead time of 100 ns. Spectra have 1024 points with an initial value of T of 24 ns and increments of 8 ns. Measurements were made using $\tau = 128$ ns to suppress ^1H modulation except where otherwise stated. Measurements were made using pulse train shot repetition rates of 10, 20, and 100 Hz. Spectra shown were obtained at 100 Hz to improve the signal-to-noise ratio. No obvious qualitative difference in the spectra was observed at the different rates at the field position for the spectra shown. Individual spectra were recorded over a period of about 1 h and summed to avoid loss of data due to temperature fluctuations which may occur over long time periods.

Before Fourier transformation the data were subject to a magnitude calculation, the echo decay was factored out by subtraction of a polynomial function, high-frequency noise was reduced with an exponential apodizing filter function, and the data set was zero filled to increase FT resolution (see, for example, refs *26* and *27*). The decay constant of the apodizing filter function was set to the minimum (2 μs) which gave a smooth transition at 8 μs to the zero-filled region, so eliminating spurious contributions from the discontinuity to the Fourier-transformed spectra. This results in an effective line broadening in the FT spectra of less than 0.1 MHz. Spectra are displayed in the power mode, which eliminates phase problems due to the dead time but may distort FT amplitude and emphasize minor intensity variations.

Spectra for each group of samples were collected under identical spectrometer conditions. Subtractions of light and dark spectra and ratios were done with the time domain data prior to Fourier transformation.

RESULTS AND DISCUSSION

The 200 K illumination of samples in the S_1 state results in conversion to the S_2 state. This is detected as the appearance of the multiline signal in CW EPR spectra or as an increase in absorption intensity in ESE spectra (Figure 1). The use of high power pulses in the ESE experiment

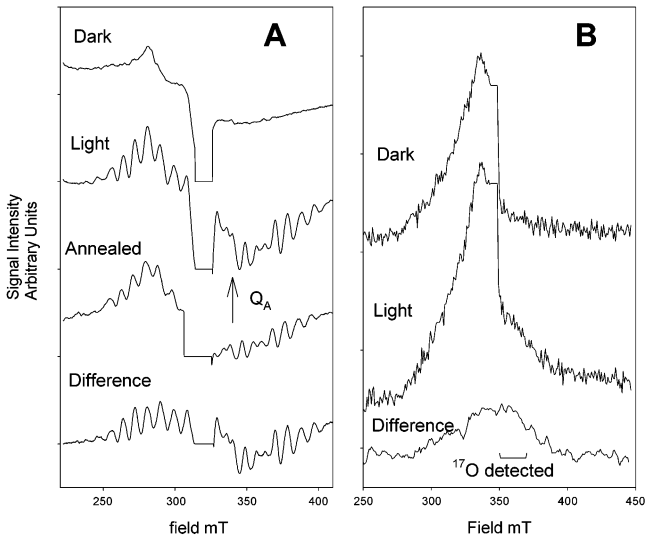

FIGURE 1: (A) CW EPR spectra of the dark background and S_2 multiline signals produced in PSII membrane samples by 200 K illumination and illumination followed by brief annealing at 273 K (see text). The position of the Q_A^- region at $g = 1.9$ is indicated. The Q_A^- signal is undetectable in the annealed sample, which still retains ~60% of the multiline signal intensity seen before annealing. (B) ESE field-swept spectra of the dark background and 200 K illuminated samples as in (A). The low-resolution difference spectrum, corresponding to the total multiline species present, is also shown. The upfield region in which ^{17}O modulation is detectable is indicated. Spectrometer conditions: (A) $T = 7$ K, microwave power 10 mW, modulation amplitude 2 mT, and frequency 9.05 GHz ($g = 2.0$ is at 323.3 mT); (B) $T = 4$ K, frequency = 9.71 GHz ($g = 2.0$ is at 346.9 mT), and shot repetition rate 100 Hz. In both (A) and (B) the large signal at $g = 2.00$ due to Y_D has been deleted for clarity.

means the resolution of the spectrum is low and the hyperfine lines seen in the CW multiline cannot be seen. The ESE spectrum shows considerable absorption in the S_1 state on the low-field side of $g = 2.00$ but little on the high-field side. In part, at least that absorption reflects signals from cytochrome b_{559} and Cu also seen in the CW spectrum. Even in the S_2 state the absorption on the high-field side of $g = 2.00$ is not intense, and the echo intensity in the ESEEM experiment is weak, requiring long data acquisition times.

Three-pulse ESEEM spectra were recorded from samples prepared from the same photosystem II preparation in $H_2{}^{16}O$ and $H_2{}^{17}O$ in the S_1 state, and then the S_2 state was induced by 200 K illumination (Figure 2). In the FT spectra (Figure 3) it is clear that modulation can be seen in the S_2 sample in $H_2{}^{17}O$ in the 2 MHz region, around the Larmor frequency of ^{17}O, which is not present in the other spectra. Preparation of light minus dark difference spectra for samples in ^{16}O water and samples in ^{17}O-enriched water (Figure 3) from the Fourier-transformed spectra again clearly show that ^{17}O-related modulation can be identified. This is more clearly seen in the $H_2{}^{17}O/H_2{}^{16}O$ ratio spectrum of the light minus dark spectra (Figure 4), when the nitrogen modulation attributed to a histidine ligand to the Mn complex (28) present in both the samples is removed. The identification of the modulation around 2 MHz as arising from ^{17}O is strengthened by measurements at τ values of 248 ns, which enhances the modulation at 2 MHz and at 496 ns which suppresses modulation at 2 MHz (Figure 5). These spectra have poorer signal-to-noise ratios than those in Figure 3 as the echo intensity at these long τ values is very small.

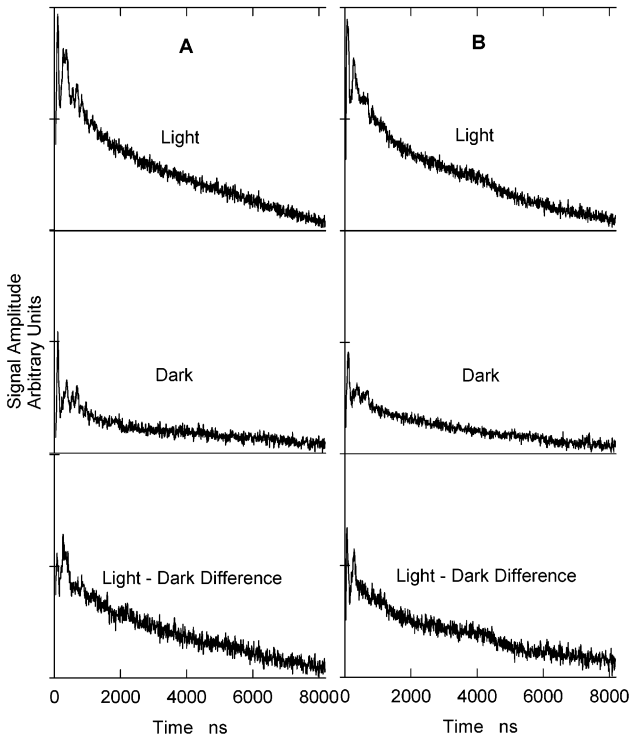

FIGURE 2: Time domain three-pulse ESEEM spectra of dark background and freshly 200 K illuminated PSII membrane samples as in Figure 1: (A) samples containing ~30% enriched ^{17}O water; (B) control samples with ^{16}O water (see text). Spectrometer conditions: $T = 4$ K, field 355.0 mT, frequency 9.71 GHz ($g = 2.0$ is at 346.9 mT), shot repetition rate 100 Hz, and $\tau = 128$ ns.

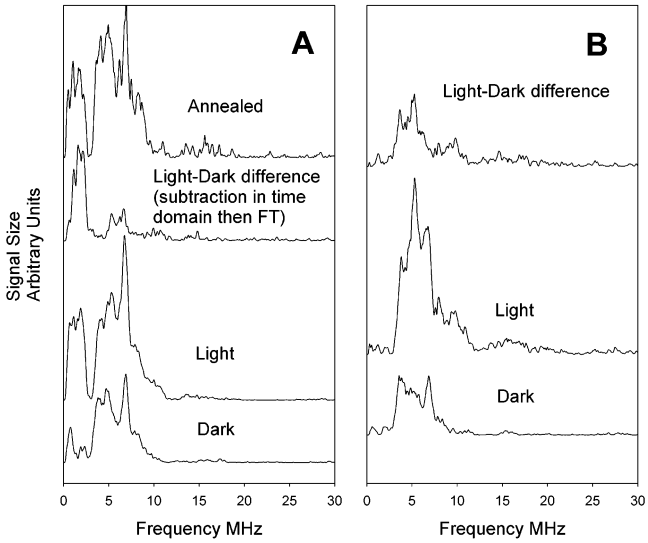

FIGURE 3: Fourier-transformed (power) spectra of the modulated components of the echo decay spectra from Figure 2: (A) ^{17}O-enriched water; (B) ^{16}O water samples. Low-frequency modulations around 1−2 MHz are clearly visible in the illuminated samples containing ^{17}O water, while illumination-induced modulation in the 4−6 MHz region, due to N, is present in both (A) and (B). In (A), ^{17}O modulation retained in the annealed sample is also shown (see text).

However, it is clear that in the $H_2{}^{17}O$ sample strong modulation is seen around 2 MHz which is absent from the $H_2{}^{16}O$ sample. The 2 MHz modulation is, as expected, suppressed in the $\tau = 496$ ns spectrum. Although not diagnostic for a specific nucleus these spectra confirm the presence of modulation in the 2 MHz region in the ^{17}O-enriched sample which is not present in the ^{16}O sample.

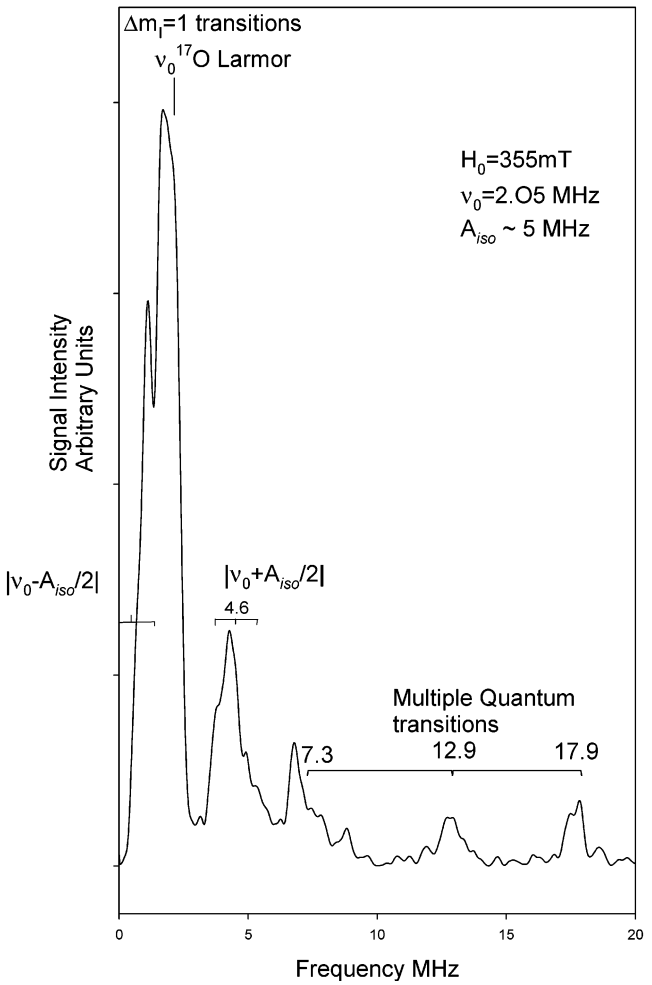

FIGURE 4: Fourier transform of the time domain ratio of light minus dark difference spectra from (A) and (B) in Figure 2 ($^{17}O/^{16}O$). This should contain only the illumination-induced ^{17}O coupling to the multiline signal (see text). The prominent low-frequency peak overlaps the ^{17}O Larmor position ($\nu_0 = 2.05$ MHz) but is not centered on it. This peak and the next most intense, centered around 4.6 MHz, are consistent with being $\nu_{\pm}$ positions of the single quantum branch transitions for a ^{17}O isotropic hyperfine coupling value (A_{iso}) of ~5 MHz. The well-resolved higher frequency overtone peaks at ~ 7, 13, and 18 MHz are then consistent with this value of A_{iso} and a quadrupole interaction term of >6 MHz (see text).

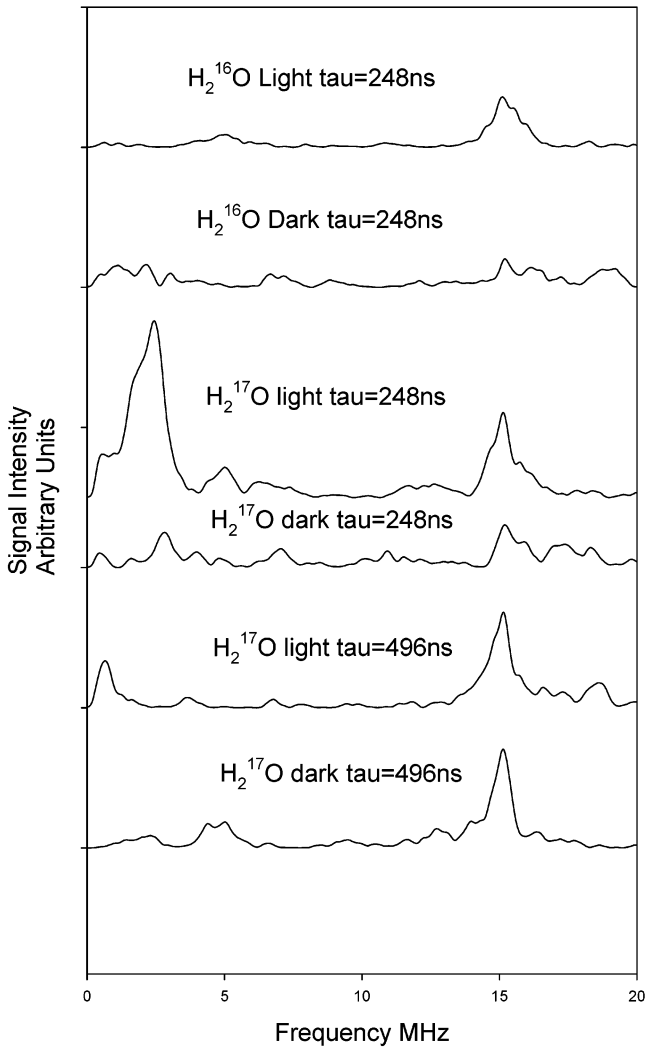

FIGURE 5: Fourier-transformed (power) spectra of the modulated components of the echo decay spectra obtained at τ values of 248 and 496 ns. $\tau = 248$ ns is expected to enhance signals around 2 MHz (^{17}O), and $\tau = 496$ ns is expected to suppress these signals. Samples prepared as described in Materials and Methods were suspended in media 30% enriched in ^{17}O water or in ^{16}O water. Spectrometer conditions: $T = 4$ K, field 355.0 mT, frequency 9.71 GHz ($g = 2.0$ is at 346.9 mT), and shot repetition rate 100 Hz.

The modulation due to ^{17}O is clearly observed in a relatively narrow field range around $g = 1.95$, between ~350−370 mT ($g = 1.98$ and $g = 1.87$). This is qualitatively similar to the case for the ^{2}H modulation seen over the central region of the multiline spectrum (*19*), but the range is significantly narrower. In Figure 1 it corresponds to the region in a "window" in which the dark background intensity is low, but the multiline envelope still has 50% or more of its maximum intensity. In fact, the $g = 1.95$ field position corresponds to the peak of the multiline absorption signal. We have not been able to detect signals on the low-field side of $g = 2.0$. It is not clear if this is because the modulation is restricted or due to the difficulty of measuring the small signals. The total echo intensity measured on the low-field side of $g = 2.0$ is much stronger than on the high-field side; however, most of that intensity is due to components other than the multiline signal. These components give rise to modulations around 1−2 MHz, which would overlap the weak ^{17}O signal and may obscure it.

As reported previously for the deuterium modulation, the signal showing ^{17}O modulation is metastable, decaying extensively on storage in the gas-phase part of a liquid nitrogen store. The signal was restored on reillumination at 200 K (data not shown), as is the case for deuterium modulation in $^{2}H_2O$ buffer and $^{2}H_3$-labeled methanol containing samples (*17*, *19*).

The appearance of the ^{17}O modulation on 200 K illumination and the decay on storage paralleling that seen for the multiline signal and deuterium modulation suggest that it associated with the multiline Mn signal. However, the restricted field range over which it is reliably detected might suggest an association with Q_A^-. We have examined this by means of an "annealing" process (*25*). In this procedure the sample is briefly thawed in the presence of the electron acceptor PPBQ and then rapidly refrozen. Q_A^- is then oxidized by the PPBQ, while the S_2 multiline is largely retained. In a number of such experiments (three samples), in which the Q_A^- signal appears to have been totally lost, we have observed that the multiline signal and the modulation

attributed to ^{17}O are partially retained (Figures 1A and 3A). These observations support the contention that the modulation is associated with the S_2 Mn signal, not Q_A^-.

Another possible source of ^{17}O modulation might be exchange of O into the bridging ligands of the Mn complex. While it is not possible to exclude this on the basis of these experiments alone, we regard it as unlikely. The current view of the Mn cluster, from EXAFS and XANES measurements, is that the Mn are organized as di-μ-oxo-bridged pairs, with a mean oxidation level of 3.5 in S_1 (*29*, *30*). Model compound data on the kinetics of bridge oxo exchange in such Mn systems appear to be sparse. However, Czernuszewicz et al. (*31*) report that in the oxo, carboxylato-bridged III−III and III−IV dimers they examined, bridge oxo exchange required protonation induced ring opening and (terminal) OH^- ligand exchange. In aqueous solution, this occurred at pH ~1. There is no evidence for such structural lability in the functional Mn cluster of PSII, especially in the lower S states. Moreover, in our case, the proton activity at the Mn site would be many orders of magnitude lower than in the exchange conditions of the model compound studies. The experiments with ^2H_2O (*19*) suggest that protons from water as well as O are close to the Mn. Britt (personal communication) has extended the analysis of ESEEM data of S_2 in ^2H_2O, using simulation of the spectra to indicate that two protons are an appropriate distance from the Mn to represent a water molecule bound through the oxygen.

The intensity of the modulation is much weaker than that observed with ^2H_2O. While this might indicate that there was less water, as opposed to exchangeable protons in the vicinity of the Mn complex, or that the O was more distant, the observation of strong hyperfine splitting of the modulation suggests the latter is unlikely. The apparent weak modulation is no doubt partly due to the low enrichment of the ^{17}O. The water used was initially 35−40% enriched; however, the photosystem II preparation was not dry. Although the sample was pelleted by centrifugation and the supernatant removed, there is no doubt the sample retained a considerable amount of ^{16}O water, which would dilute the ^{17}O. It is therefore unlikely that the final enrichment was better than 20%, or 30% in the experiment in which the sample was washed and then resuspended in the ^{17}O-enriched medium.

The difference/ratio data in Figure 4 should, to good approximation, isolate the pure ^{17}O frequency contributions to the echo modulation on the S_2 multiline signal, as the three-pulse acquisition sequence eliminates nuclear combination frequencies. Resonances up to ~18 MHz are reliably detected. Although no detailed simulation analysis on the data was performed, comparison with ^{17}O ESEEM results from other systems allows simple, semiquantitative conclusions to be drawn. Thomann et al. (*32*) have studied ^{17}O water binding to the Fe^{3+} ion in cytochrome P450 and simulated ^{17}O ESEEM spectra from an electron spin $^1/_2$ center for a range of coupling parameter values. In addition, Tan et al. (*33*) have reported ^{17}O ENDOR and ESEEM data for water binding to Mn^{2+} in frozen solution. Although the predicted responses are complex for a spin $^5/_2$ nucleus, these results show that the ESEEM powder pattern will have characteristic, partially allowed high-frequency multiple-quantum (overtone) transitions from the hyperfine coupling when the quadrupole term, e^2Qq/h, is large (>6 MHz). These are clearly visible in Figure 4 at ~7, 13, and 18 MHz. If the ^{17}O hyperfine coupling to the metal center is only moderately anisotropic, as is the case in the above examples, then the single-quantum branches occur at approximately $|A_{iso}/2 \pm \nu_0|$, as for the case with simple spin $^1/_2$ systems. Here A_{iso} is the isotropic component of the hyperfine interaction and ν_0 the ^{17}O Larmor frequency. The resonances are broadened by the quadrupolar interaction. The negative branch typically overlaps the ^{17}O free resonance position from weakly coupled nuclei ($\nu_0 = 2.05$ MHz here). The peak pattern in Figure 4 fits this picture if $A_{iso} \sim 5$ MHz. This is also totally consistent with the separations of the higher frequency overtone peaks, which are approximately equal to A_{iso} under these conditions (see ref *30*). The simulations of Thomann et al. show that overtone patterns, such as seen in Figure 4 and with axial ^{17}O binding to the heme Fe $^{3+}$ in cytochrome P450, depend sensitively on the rhombicity (η, ~1 in these cases) of the ^{17}O quadrupole tensor and its orientation relative to the hyperfine tensor. The data suggest water, rather than OH^-, as the bound species, as was concluded for cytochrome P450 (*32*).

The *apparent* hyperfine coupling term (A_{iso}~ 5 MHz) for ^{17}O water bound in S_2 of the photosystem is, however, approximately twice that inferred for the water bound to the Fe^{3+} center in P450 (2.6 MHz). This could still be consistent with the *actual* A_{iso} term being essentially the *same* as in the P450 binding but with the water bound to a quasi-axial Mn(III) ion in a spin $S = {}^1/_2$ coupled Mn cluster, for which the nuclear hyperfine projection constant of the Mn(III) in the cluster state is ~2. Of published simulation studies of the S_2 state EPR spectrum, one predicts a Mn(III) spin projection of 2.0 (*34*, *36*), two values of ~1.6−1.8 (*35*, *36*), and two values close to 1.0 (*37*, *38*).

The results indicate that water binds directly to the Mn through oxygen. As with our experiments with ^2H_2O, two multiline components are detected, only one of which shows detectable modulation.

ACKNOWLEDGMENT

We are grateful to Paul Smith for extensive discussion of the data analysis procedures. We acknowledge helpful comments from a referee for an earlier version of this paper.

REFERENCES

1. Nugent, J. H. A., Ed. (2001) *Biochim. Biophys. Acta 1503*, 1−259.
2. Joliot, P., Barbieri, G., and Chaboud, R. (1969) *Photochem. Photobiol. 10*, 309−329.
3. Kok, B., Forbush, B., and McGloin, M. (1970) *Photochem. Photobiol. 11*, 457−475.
4. Yachandra, V. K., Derose, V. J., Latimer, M. J., Mukerji, I., Sauer, K., and Klein, M. P. (1992) *Science 260*, 675−679.
5. MacLachlan, D. J., Nugent, J. H. A., Bratt, P. J., and Evans, M. C. W. (1994) *Biochim. Biophys. Acta 1186*, 186−200.
6. Messinger, J., Nugent, J. H. A., and Evans, M. C. W. (1997) *Biochemistry 36*, 11055−11060.
7. Ahrling, K. A, Peterson, S., and Styring, S. (1997) *Biochemistry 36*, 13148−13152, 6366.
8. Geiger, P., Petersen, S., Åhrling, K. A., Deák, Z., and Styring, S. (2001) *Biochim. Biophys. Acta 1503*, 83−95.
9. Dismukes, G. C., and Siderer, Y. (1981) *Proc. Natl. Acad. Sci. U.S.A. 78*, 274−278.
10. Dexheimer, S. L., and Klein, M. P. (1992) *J. Am. Chem. Soc. 114*, 2821−2826.
11. Matsukawa, T., Mino, H., Yoneda, D., and Kawamori, A. (1999) *Biochemistry 38*, 4072−4077.
12. Messinger, J., Hillier, W., and Wydrzynski, T. (1998) *Biochemistry 37*, 16908−16914.

13. Hendry, G., and Wdrzynski, T. (2002) *Biochemistry 41*, 13328−13334.
14. Andreasson, L.-E. (1998) *Biochim. Biophys. Acta 973*, 465−467.
15. Nugent, J. H. A. (1987) *Biochim. Biophys. Acta 893*, 184−189.
16. Turconi, S., Maclachlan, D. J., Bratt, P. J., Nugent, J. H. A., and Evans, M. C. W. (1997) *Biochemistry 36*, 879−885.
17. Evans, M. C. W., Gourovskaya, K., and Nugent, J. H. A. (1999) *FEBS Lett. 450*, 285−288.
18. Force, D. A., Randall, D. W., Lorrigan, G. A., Clemens, K. L., and Britt, R. D. (1998) *J. Am. Chem. Soc. 120*, 13321−13333.
19. Evans, M. C. W., Rich, A. M., and Nugent, J. H. A. (2000) *FEBS Lett. 477*, 113−117.
20. Britt, R. D., Peloquin, J. M., and Campbell, K. A. (2000) *Annu. Rev. Biophys. Biomol. Struct. 299*, 463−495.
21. Smith, P. J., and Pace, R. J. (1993) *J. Chem. Soc., Farad*ay *Trans. 89*, 2863−2868.
22. Boussac, A. (1997) *J. Biol. Inorg. Chem. 2*, 580−585.
23. Ford, R. C., and Evans, M. C. W. (1983) *FEBS Lett. 160*, 159−164.
24. Porra, R. J., Thompson, W. A., and Kriedemann, P. E. (1989) *Biochim. Biophys. Acta 975*, 384−394.
25. Nugent, J. H. A., Turconi, S., and Evans, M. C. W. (1997) *Biochemistry 36*, 7086−7096.
26. Davis, I. H., Heathcote, P., MacLachlan, D. J., and Evans, M. C. W. (1993) *Biochim. Biophys. Acta 1143*, 183−189.
27. Bebetis, N. P., Dave, P. C., and Goldfarb, D. (2002) *J. Magn. Reson. 158*, 126−142.
28. Tang, X.-S., Diner, B. A., Larsen, B. S., Gilchrist, M. L., Lorigan, G. A., and Britt, R. D. (1994) *Proc. Natl. Acad. Sci. U.S.A. 91*, 704−708.
29. Robblee, J. H., Cinco, R. M., and Yachandra, V. K. (2001) *Biochim. Biophys. Acta 1503*, 7−23.
30. Dau, H., Iuzzolino, L., and Dittmer, J. (2001) *Biochim. Biophys. Acta 1503*, 24−39.
31. Czernuszewicz, R. S., Dave, B., and Rankin, J. G. (1991) in *Spectroscopy of Biological Molecules* (Hester, R. E., and Girling, R. B., Eds.) pp 284−288, Royal Society of Chemistry, Cambridge, U.K.
32. Thomann, H., Bernardo, M., Goldfarb, D., Kroneck, P. M. H., and Ullrich, V. (1995) *J. Am. Chem. Soc. 117*, 8243−8251.
33. Tan, X., Bernardo, M., Thomann, H., and Scholes, C. P. (1993) *J. Phys. Chem. 98*, 5147−5157.
34. Åhrling, K. A., and Pace, R. J. (1995) *Biophys. J. 68*, 2081−2090.
35. Peloquin, J. M., Campbell, K. A., Randall, D. W., Evanchik, M. A., Pecoraro, V. L., Armstrong, W. H., and Britt, R. D. (2000) *J. Am. Chem. Soc. 122*, 10926−10942.
36. Zheng, M., and Dismukes, G. C. (1996) *Inorg. Chem. 35*, 3307−3319.
37. Hasegawa, K., Kusonoki, M., Inoue, Y., and Ono, T.-a. (1998) *Biochemistry 37*, 9457−9465.
38. Lakshmi, K. V., Eaton, S. S., Eaton, G. R., Frank, H. A., and Brudvig, G. W. (1999) *J. Phys. Chem. B 102*, 8327−8335.

BI035489Y